A Lys−Trp Cation−π Interaction Mediates the Dimerization and Function of the Chloride Intracellular Channel Protein 1 Transmembrane Domain

ARTICLE *in* BIOCHEMISTRY · DECEMBER 2013

Impact Factor: 3.02 · DOI: 10.1021/bi401433f

4 AUTHORS, INCLUDING:

Anton Polyansky
University of Vienna
38 PUBLICATIONS **422** CITATIONS
SEE PROFILE

Sylvia Fanucchi
University of the Witwatersrand
13 PUBLICATIONS **101** CITATIONS
SEE PROFILE

Heini Dirr
University of the Witwatersrand
89 PUBLICATIONS **2,773** CITATIONS
SEE PROFILE

BIOCHEMISTRY
including biophysical chemistry & molecular biology

Article

pubs.acs.org/biochemistry

A Lys−Trp Cation−π Interaction Mediates the Dimerization and Function of the Chloride Intracellular Channel Protein 1 Transmembrane Domain

Bradley Peter,[†] Anton A. Polyansky,[‡,§] Sylvia Fanucchi,[†] and Heini W. Dirr*[,†]

[†]Protein Structure-Function Research Unit, School of Molecular and Cell Biology, University of the Witwatersrand, Johannesburg 2050, South Africa

[‡]Department of Structural and Computational Biology, Max F. Perutz Laboratories, University of Vienna, Campus Vienna Biocenter 5, Vienna AT-1030, Austria

[§]M. M. Shemyakin and Yu. A. Ovchinnikov Institute of Bioorganic Chemistry, Russian Academy of Sciences, Moscow 117997, Russia

Supporting Information

ABSTRACT: Chloride intracellular channel protein 1 (CLIC1) is a dual-state protein that can exist either as a soluble monomer or in an integral membrane form. The oligomerization of the transmembrane domain (TMD) remains speculative despite it being implicated in pore formation. The extent to which electrostatic and van der Waals interactions drive folding and association of the dimorphic TMD is unknown and is complicated by the requirement of interactions favorable in both aqueous and membrane environments. Here we report a putative Lys37−Trp35 cation−π interaction and show that it stabilizes the dimeric form of the CLIC1 TMD in membranes. A synthetic 30-mer peptide comprising a K37M TMD mutant was examined in 2,2,2-trifluoroethanol, sodium dodecyl sulfate micelles, and 1-palmitoyl-2-oleoyl-*sn*-glycero-3-phosphocholine liposomes using far-ultraviolet (UV) circular dichroism, fluorescence, and UV absorbance spectroscopy. Our data suggest that Lys37 is not implicated in the folding, stability, or membrane insertion of the TMD peptide. However, removal of this residue impairs the formation of dimers and higher-order oligomers. This is accompanied by a 30-fold loss of chloride influx activity, suggesting that dimerization modulates the rate of chloride conductance. We propose that, within membranes, individual TMD helices associate via a Lys37-mediated cation−π interaction to form active dimers. The latter findings are also supported by results of modeling a putative TMD dimer conformation in which Lys37 and Trp35 form cation−π pairs at the dimer interface. Dimeric helix bundles may then associate to form fully active ion channels. Thus, within a membrane-like environment, aromatic interactions involving a polar lysine side chain provide a thermodynamic driving force for helix−helix association.

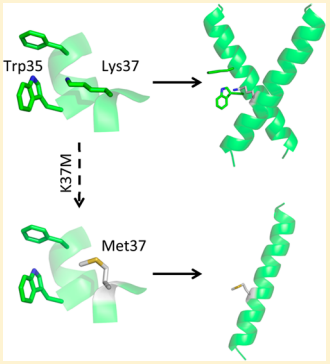

The two-step folding model proposed by Popot and Engelman[1,2] and the modified two-step model of White and Wimley[3] have been used to explain the mechanisms by which membrane proteins bind to, insert, and oligomerize in membranes. These models depict TMDs as independently stable and folded units capable of self-association. The self-association of transmembrane helices is a key step in membrane protein folding because it typically results in the protein adopting a functional form. Helix−helix association is thought to be mediated largely through noncovalent van der Waals and electrostatic forces.[4] The former utilizes small residue packing motifs to maximize helix contacts, such as GxxxG[5] and AxxxA,[6] whereas electrostatic interactions occur between polar side chains and side chain and backbone residues of interacting helices.[7−9] Although these two interactions predominate, other important subsets of noncovalent interactions involving aromatic residues exist. These may involve (i) two aromatic residues (π−π stacking) or (ii) a basic and an aromatic residue (cation−π). The latter is emerging as an important stabilizing force in membrane proteins,[10−12] being favorable in a hydrophobic medium[13−15] with an average strength of −6.5 kcal/mol.[16] The extent to which cation−π interactions direct membrane protein folding and transmembrane helix association is poorly understood, given that the energetics associated with the polar and aromatic groups differ substantially between membrane and water-soluble proteins.

Proteins capable of adopting multiple stable native states present an intriguing variation to these schemes. These proteins undergo large-scale structural rearrangements upon association with the lipid bilayer, resulting in the spontaneous conversion from a water-soluble to a membrane-bound form.[17] This requires interactions that are favorable in both aqueous and membrane environments, limiting the ensemble of potential helix−helix contacts. The eukaryotic chloride intracellular channel (CLIC) protein family is an example of a class of

Received: October 22, 2013
Revised: December 11, 2013
Published: December 11, 2013

   dx.doi.org/10.1021/bi401433f | *Biochemistry* 2014, 53, 57−67

amphitropic proteins that have evolved to overcome this limitation.

In their reduced monomeric state, the CLIC proteins adopt a topology similar to that of the GST superfamily, with a thioredoxin N-domain and an all-α-helical C-domain (Figure 1A).[18] CLICs are unique among all eukaryotic ion channels in

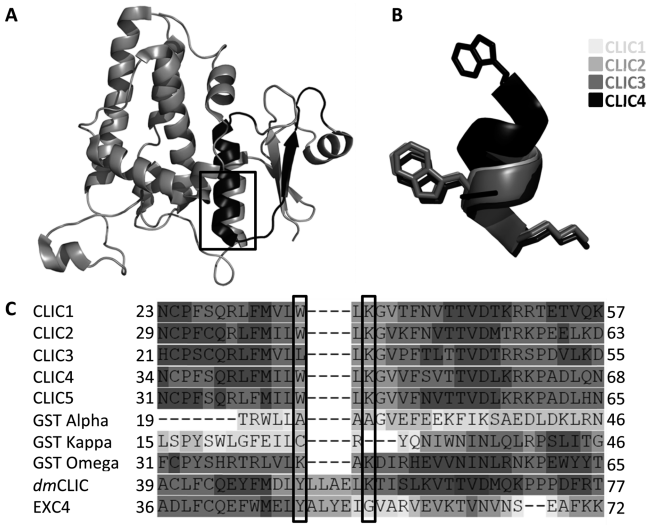

Figure 1. Structure and sequence conservation of the CLIC1 TMD. (A) The CLIC1 TMD comprises residues 24–46, which include most of helix α1 and sheet β2 (black) of the N-domain. This region shows strong sequence conservation across the vertebrate CLICs as well as the invertebrate homologues Exc4 (*Caenorhabditis elegans*) and dmCLIC (*Drosophila melanogaster*). The residues involved in a putative cation–π interaction are superimposed in panel B and boxed in panel C.

that they are dimorphic and can exist in either a soluble or membrane-bound form.[18] The best characterized member of this family is the p64 homolgue CLIC1. The soluble–membrane transition of CLIC1 likely involves the exposure of a single TMD. We have demonstrated that the isolated TMD undergoes structural modifications in a membrane environment, including the acquisition of helical secondary structure and dimerization.[19] Although the residues involved in dimerization are unknown, it is likely that they form noncovalent helix–helix interactions. The oligomerization process, which completes the two-step folding model, has been poorly characterized in CLIC1. To date, two models for the functional CLIC1 channel have been proposed.[20,21] However, neither of these models provides any indication about which interactions stabilize the TMD oligomers in the membrane. Modeling of the CLIC1 TMD dimer has identified a putative cation–π interaction at the dimer interface. This interaction, along with a network of hydrophobic contacts, may play an important role in stabilizing the dimer and higher-order oligomers in the membrane. This has both structural and functional implications, given that the single TMD of CLIC1 alone is insufficient to form an ion-conducting membrane channel.

To improve our understanding of the process of oligomerization in CLIC1, we probed the role of Lys37 as a key residue in maintaining the specificity and stability of dimerization in the TMD. In this study, we examined the secondary, tertiary, and quaternary structural changes of a K37M CLIC1 TMD mutant as it partitions between an aqueous and membrane-mimicking environment.

MATERIALS AND METHODS

Modeling of TMD Dimer Conformations. The CLIC1 TMD sequence (Figure 1) was built into uniform α-helices with ideal backbone torsion angles of −65° (φ) and −40° (ψ) using Chimera version 1.6.2. Side chain rotamers were chosen using the backbone-dependent rotamer library program SCWRL.[22] Subsequently, the dimeric structure of the CLIC1 TMD was reconstructed using the PREDDIMER algorithm (http://model.nmr.ru/preddimer/).[23] Packing efficiencies of the predicted conformations were estimated according to the PREDDIMER scoring function (F_{SCOR}).

Peptide Design and Synthesis. The 30-residue CLIC1 K37M TMD peptide (22-GNCPFSQRLFMVLWLMGVTFN-VTTVDTKRR-51) containing a carboxylated amino terminus and an amidated carboxyl terminus was synthesized using a solid phase continuous flow system by GL Biochem (Shanghai, China). Its purity was determined to be >95% using high-performance liquid chromatography.

Sample Preparation. Samples were solubilized in 100% (v/v) methanol to yield a 1 mM stock solution and prepared as previously described.[19] Incorporation of the peptide into SDS micelles and POPC liposomes was conducted according to an established protocol.[19] Lucigenin-encapsulated liposomes were prepared using a method identical to that described previously[19] with the inclusion of 10 mM Lucigenin (Sigma-Aldrich) and 15 mM potassium acetate in reconstitution buffer. Free Lucigenin was removed by size-exclusion chromatography on a Sephadex G-25 column equilibrated with reconstitution buffer.

CD and Fluorescence Spectroscopy. Far-UV CD and fluorescence spectra of the K37M peptide were recorded in TFE, SDS, and POPC as described previously.[19] Spectra were buffer-corrected and smoothed using the negative exponential method. CD spectra were normalized to mean residue ellipticity ($[\theta]$) using the equation

$$[\theta] = (100\theta)/(cnl)$$

where $[\theta]$ is the molar ellipticity (degrees square centimeter per decimole), θ is the ellipticity (millidegrees), c is the protein concentration (millimolar), n is the number of residues in the peptide, and l is the path length (centimeters). For all far-UV CD analyses, n = 30 and l = 0.1 cm. A quantitative estimation of the secondary structure content of the TMD peptide was made using the CDPro software package as described previously.[19,24] The standard error of the secondary structural elements was determined from four separate CDPro analyses.

To analyze the effect of oxidation, 10 μM peptide was incubated with 2 mM H_2O_2 for 0–24 h and analyzed as previously described.[19] Acrylamide and iodide quenching was also performed as described previously.[19] The fluorescence intensity at 345 nm was monitored and analyzed according to the Stern–Volmer relationship:

$$F_0/F = 1 + K_{SV}[Q]$$

where F_0 and F are the emission intensities in the absence and presence of the quencher, respectively, [Q] is the concentration of the quencher, and K_{SV} is the Stern–Volmer constant.

DTNB Assay. DTNB (5,5′-dithio-2-nitrobenzoic acid) is a water-soluble compound used to quantify free thiol (-SH) groups in solution based on their solvent accessibility. The

dx.doi.org/10.1021/bi401433f | *Biochemistry* 2014, 53, 57–67

CLIC1 K37M TMD contains a single cysteine residue at position 24. The DTNB assay was performed as described previously[19] in SDS and POPC. In the case of liposome samples, two versions of the DTNB assay were performed: (i) as described above with extrinsic DTNB added to samples and (ii) using DTNB encapsulated within the liposomes. The aim of these two methods was to probe whether Cys24 is located at the *cis* or *trans* face of the membrane mimetic. The concentration of 2-nitro-5-thiobenzoic acid (NTB) was determined spectrophotometrically at 412 nm using an extinction coefficient of 13600 M^{-1} cm^{-1}.[25] The proportion of free thiols was obtained from the ratio of NTB concentration to peptide concentration.

Tricine Sodium Dodecyl Sulfate–Polyacrylamide Gel Electrophoresis (SDS–PAGE). The oligomeric state of the K37M TMD peptide in SDS micelles was investigated by gel electrophoresis. A modified Tricine buffer system[26] with a 0.5% SDS gel was used. Samples were prepared and electrophoresed as described previously.[19] A dimer control was included by incubating samples with 2 mM H_2O_2 in the absence of β-mercaptoethanol, thereby inducing the formation of a Cys24–Cys24 disulfide bond between two peptides. Silver staining was performed using the SilverQuest kit (Life Technologies, Carlsbad, CA) according to the manufacturer's instructions. Band intensities were quantified using ImageJ (http://rsbweb.nih.gov/ij/).

UV Absorption. To probe whether a cation–π interaction occurs between Lys37 and Phe41/Trp35, UV absorption spectra of the wild-type and K37M peptides were recorded. This method of detecting cation–π interactions is based on the weakening of the B_b tryptophan absorbance (at ~220 nm) accompanied by a red shift to ~230 nm in the presence of these interactions.[27,28] The negative–positive peak pair at 220/230 nm is considered a marker of tryptophan residues involved in cation–π interactions. Samples of 10 μM wild-type or K37M peptides were analyzed in buffer [20 mM sodium phosphate and 1 mM DTT (pH 5.5)], 40% (v/v) TFE, or 15 mM SDS. Spectra were recorded between 200 and 300 nm in a 1 cm quartz cuvette using a Jasco V-630 spectrophotometer (Jasco, Tokyo, Japan) at 20 °C and are an average of three accumulations. Spectra were buffer-corrected and plotted as the difference between the SDS and TFE spectra (SDS – TFE). The TFE spectra serve as controls for no interaction as TFE inhibits quaternary contacts.[29]

Chloride Influx Assay. To determine whether (i) the TMD peptide has been functionally reconstituted into membranes and (ii) dimerization is required for function, a method for monitoring the movement of chloride ions across a phospholipid bilayer was developed. The assay is based on the quenching of an encapsulated chloride-sensitive fluorescent dye Lucigenin by extravesicular chloride ions.

Wild-type or K37M TMD peptides were mixed with Lucigenin-encapsulated liposomes (see Sample Preparation) and left to equilibrate covered for 2 h. The final lipid concentration was 2.5 mM, and final peptide concentrations were between 2 and 50 μM. Blank samples were supplemented with appropriate volumes of 100% (v/v) methanol. The CLIC1 activity has previously been shown to be pH-sensitive.[30] Therefore, samples were analyzed at either (i) pH 7.2, the pH of the cytosol, or (ii) pH 5.5, the pH at the membrane surface. Fluorescence emission spectra of the encapsulated dye were recorded between 400 and 600 nm in a 1 cm quartz cuvette using a Perkin-Elmer LS50B luminescence spectrometer (Perkin-Elmer, Waltham, MA) at 20 °C and are an average of five accumulations. An excitation wavelength of 368 nm, a scan speed of 250 nm/min, and 3.5 nm slit widths were used. Peptide samples were prepared and analyzed in 20 mM sodium phosphate, 15 mM potassium chloride, 1 mM DTT, and 0.02% sodium azide (pH 5.5 or 7.2). The percent quenching following the addition of 4 μM valinomycin was determined according to

$$(1 - F_{484P}/F_{484B}) \times 100\%$$

where F_{484P} and F_{484B} represent the emission intensity at 484 nm in the presence and absence of the TMD peptide, respectively. The kinetics of chloride influx was monitored at 484 nm as described, following the addition of 20 μM wild-type or K37M TMD peptide. Data were fit to either a single- or double-exponential decay model in SigmaPlot version 11.0 from which the observed rate constants (k_{obs}) were derived.

RESULTS

Predicted Structure of the CLIC1 TMD Dimers. We have previously demonstrated that the CLIC1 TMD forms stable dimers in membrane mimetics.[19] The putative conformation of the dimer was predicted by the PREDDIMER algorithm[23] (Figure 2). This model has the top-ranking score (F_{SCOR} = 3.1) among other possible variants and represents the

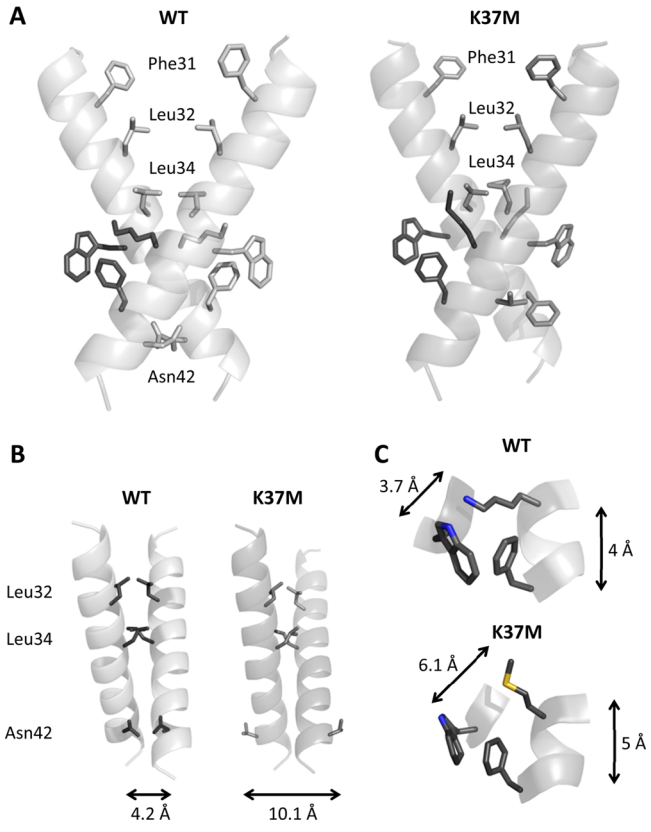

Figure 2. Modeled structure of the CLIC1 TMD dimers. (A) The dimeric wild-type and K37M CLIC1 TMD was modeled using the PREDDIMER algorithm.[23] The interacting helices cross at an angle of 60° to form a symmetric dimer ~32 Å in length. The dimer interface comprises a network of hydrophobic residues (B) as well as a cation–π interaction between Lys37 and Trp35/Phe41 (C). The C_α–C_α distances between Asn42 and Asn42, Trp35 and Lys37/Met37, and Phe41 and Lys37/Met37 are shown. All figures were rendered using PyMol version 1.3.

dx.doi.org/10.1021/bi401433f | *Biochemistry* 2014, 53, 57–67

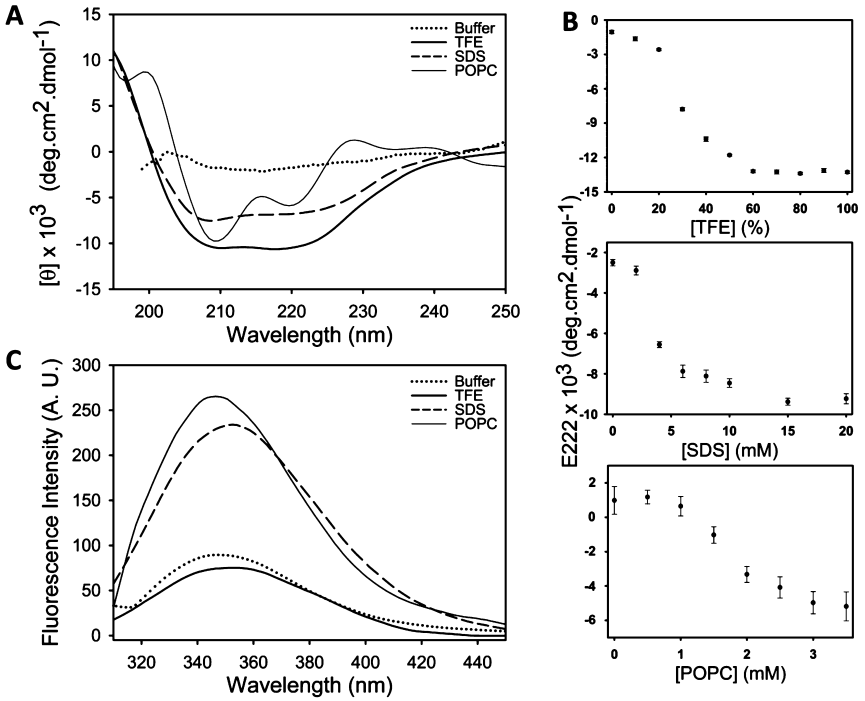

Figure 3. Secondary and tertiary structure of the CLIC1 K37M TMD peptide. Far-UV CD (A and B) and tryptophan fluorescence (C) spectra were recorded in buffer (dotted), in 40% (v/v) TFE (thick solid), in 15 mM SDS micelles (dashed), and in 2.5 mM POPC (thin solid). (A) In solution, the peptide is unstructured, whereas the addition of TFE, SDS, and POPC induces α-helical secondary structure. (B) The helical content of 15 μM peptide is maximal at 60% (v/v) TFE, 15 mM SDS, and 3 mM POPC, after which no further increase in helicity is observed. (C) In TFE, the peptide emits maximally at 353 nm, whereas SDS and POPC induce both a blue-shifted λ_{max} (346 and 339 nm) and a 2.5-fold increase in emission intensity. This indicates that Trp35 becomes located in a hydrophobic environment, presumably inserted into the SDS micelles or POPC liposomes. The buffer consisted of 20 mM sodium phosphate, 1 mM DTT, and 0.2% (w/v) sodium azide (pH 5.5). Error bars represent the standard deviation from four independent replicates.

dimer with the best packing efficiency. The model comprises TMD residues 22−46 with a total hydrophobic length of ∼32 Å. The helices form a symmetric right-handed dimer with a crossing angle of −60°. The dimer interface comprises a series of hydrophobic interactions that include Phe31, Leu32, Leu34, and Asn42. In addition, a cation−π interaction between Lys37 and Trp35 was identified. The residues involved in this interaction are conserved across the vertebrate CLICs as well as the *Drosophila melanogaster* CLIC homologue (Figure 1C). On the basis of this model, we created the K37M TMD mutant to probe whether the predicted cation−π interaction was involved in dimer formation and/or stabilization. The K37M TMD dimer has packing properties similar to those of the wild type (Figure 2A). However, the rotational angle of the helices is asymmetric compared to that of the wild type, which results in the loss of contact between Asn42 residues on opposite chains (Figure 2B). The proximity of Met37 to both Trp35 and Phe41 is also reduced (Figure 2C) compared to that of the wild type.

Secondary Structure Content. The far-UV CD spectra of the K37M TMD peptide in aqueous buffer, TFE, SDS micelles, and POPC liposomes are shown in Figure 3. In solution, the peptide is unstructured. Upon addition of TFE, SDS micelles, or POPC liposomes, the CD spectra exhibit two minima near 208 and 222 nm, which is characteristic of a predominantly α-helical conformation. Much like that of the wild-type peptide, the spectra in POPC displayed an additional maximum at ∼228 nm that can be attributed to aromatic side chains adopting an ordered conformation.[31] In addition, the molar ellipticity of the K37M TMD peptide in TFE was 25 ± 4% and 12 ± 2% higher than that in SDS micelles and POPC liposomes, respectively. This suggests that a greater proportion of peptide assumes an α-helical conformation under these conditions compared to a micellar/vesicle environment. Quantitative secondary structure analysis of the wild-type and K37M peptides is summarized in Table 1. Both peptides show a similar trend, with membrane mimetics inducing an increase in α-helical content and decreases in β-structure and unordered structure content (Table 1). The α-helical content of the K37M peptide increased sigmoidally with increasing TFE, SDS, and POPC concentrations, reaching a maximum at 60% (v/v) TFE, 15 mM SDS, or 3 mM POPC (Figure 3B). Compared to the wild-type peptide (see Table 1), the K37M mutant requires an additional 20% (v/v) TFE or 0.5 mM POPC to achieve maximal helicity. The thermal stability of the peptide was also analyzed by measuring the ellipticity at 222 nm in 40% TFE or 15 mM SDS at increasing temperatures (Figure S1 of the Supporting Information). Both the wild-type and K37M peptides unfolded via noncooperative and fully reversible pathways. The sequential, rather than simultaneous, disruption of amide hydrogen bonds resulting in this behavior is characteristic of transmembrane helices.[32]

Tertiary Structure. The K37M TMD peptide contains a lone tryptophan residue at position 35 that can be used as a reporter of local tertiary structural changes. In solution, the peptide exhibits a fluorescence emission spectrum with a low emission intensity and a maximal emission wavelength (λ_{max}) of 349 nm (Figure 3C). The introduction of a methionine at position 37 has caused a 6 nm blue shift of the λ_{max} compared to that of the wild-type peptide (see Table 1). In the presence of TFE, the emission intensity was reduced by ∼25% while

dx.doi.org/10.1021/bi401433f | *Biochemistry* 2014, 53, 57−67

Table 1. Structural Changes of the Wild-Type and K37M CLIC1 TMD Peptides in Response to Membrane Mimetics[a]

	buffer	TFE	SDS	POPC
α-helix (%)[b]	18 ± 5	64 ± 8	59 ± 10	56 ± 9
	17 ± 6	67 ± 9	60 ± 3	61 ± 5
β-sheet (%)[b]	23 ± 4	9 ± 2	7 ± 3	11 ± 6
	25 ± 6	8 ± 4	7 ± 4	8 ± 3
random coil (%)[b]	56 ± 9	22 ± 9	29 ± 7	31 ± 11
	54 ± 7	21 ± 5	31 ± 6	28 ± 9
NRMSD	0.23	0.095	0.11	0.17
	0.19	0.104	0.096	0.14
λ_{max} (nm)	355 ± 2	355 ± 1	343 ± 1	342 ± 3
	349 ± 3	353 ± 2	346 ± 3	339 ± 2
K_{SV} (M^{-1})[c]	15.35 ± 0.23, 3.52 ± 0.12	ND[e]	5.66 ± 0.1, 1.03 ± 0.09	7.01 ± 0.76
	8.6 ± 0.16, 2.53 ± 0.13	ND[e]	2.42 ± 0.08, 1.08 ± 0.13	2.79 ± 0.09
fraction of free thiols[d]	0.98 ± 0.01	ND[e]	0.64 ± 0.009	0.39 ± 0.01, 0.63 ± 0.03
	1 ± 0.02	ND[e]	0.67 ± 0.012	0.4 ± 0.011, 0.61 ± 0.014
thermal unfolding	ND[e]	linear	linear	ND[e]
	ND[e]	linear	linear	ND[e]

[a]Wild-type values are shown first. The results for the wild type have been published previously.[19] The standard deviation from four independent replicates is given. [b]CDPro reference set SP43. [c]Samples with two values represent the K_{SV} determined from acrylamide and iodide quenching, respectively. [d]In POPC, the first value represents external DTNB (*cis*) while the second value represents encapsulated DTNB (*trans*). [e]Not determined.

shifting the λ_{max} to 353 nm. Both SDS and POPC induced a blue-shifted λ_{max} (346 and 339 nm) and a 2.5-fold increase in emission intensity. This behavior is similar to that of the wild type and suggests that Trp35 of the TMD peptide is inserted into the SDS micelles or POPC liposomes. The local environment of Trp35 may also be influenced by quaternary interactions in addition to interactions with the mimetics, particularly if Trp35 is located at or near an oligomer interface.

We have previously demonstrated that, under oxidizing conditions, the emission spectra of Trp35 are quenched by H_2O_2 on the basis of solvent accessibility.[19] This is a result of the conversion of the indole ring to oxyindole over time. As with the wild-type peptide, the K37M peptide shows ∼5% quenching in SDS and POPC, ∼20% quenching in TFE, and ∼30% quenching in solution over 24 h (Figure 4C). This reflects the nature of the mimetic, with the peptide being inserted into the POPC liposomes or SDS micelles and partially shielded by the TFE. The overall levels of quenching in the K37M peptide are, on average, 10−20% lower than in the wild type. This correlates well with the λ_{max} values that are blue-shifted relative to that of the wild-type peptide.

Solvent Accessibility of Trp35 and Cys24 in SDS Micelles or POPC Liposomes. The wild-type CLIC1 TMD peptide spontaneously associates with and inserts into SDS micelles or POPC liposomes.[19] To determine whether the K37M mutation interferes with this interaction, dynamic fluorescence quenching with acrylamide or iodide and a DTNB assay were conducted. Panels A and B of Figure 4, Figure S2 of the Supporting Information, and Table 1 show the Stern−Volmer constants (K_{SV}) obtained using acrylamide and iodide. This constant reflects residue accessibility, with low values indicating residues with a low level of exposure and vice versa. In the absence of membrane mimetics, both acrylamide

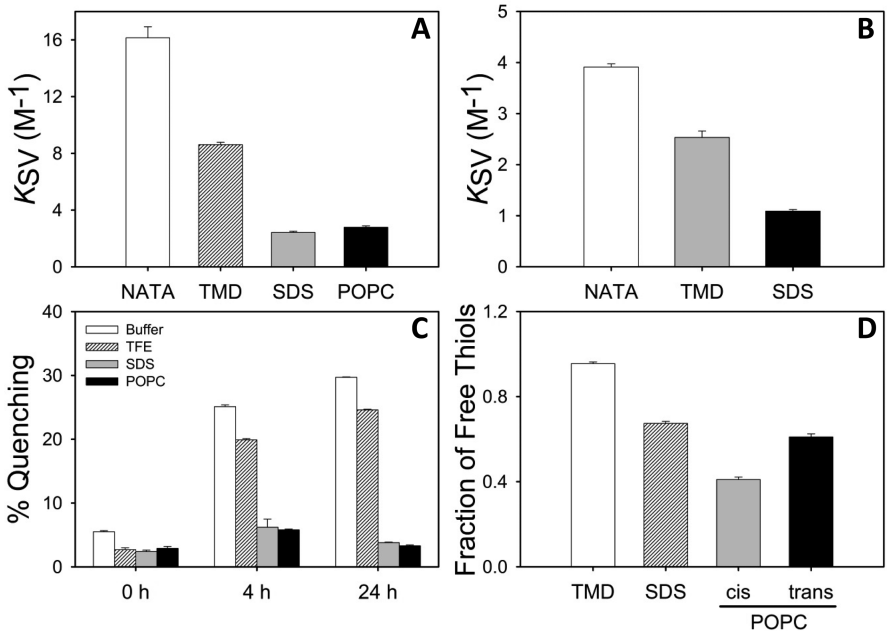

Figure 4. Solvent accessibility of the CLIC1 K37M TMD peptide in SDS micelles and POPC liposomes. Dynamic acrylamide (A), iodide (B), and H_2O_2 (C) quenching as well as a DTNB assay (D) were performed in the absence and presence of 40% (v/v) TFE (C only), 15 mM SDS, or 2.5 mM POPC. For panel C, samples were analyzed by fluorescence following the addition of 2 mM H_2O_2. In panel D, TMD refers to the free TMD peptide in solution, SDS refers to the TMD peptide inserted into SDS micelles, *cis* refers to external DTNB, and *trans* refers to encapsulated DTNB. The buffer consisted of 20 mM sodium phosphate, 1 mM DTT, and 0.2% (w/v) NaN_3 (pH 5.5) (quenching) or 20 mM Na_2PO_4, 1 mM EDTA, and 0.2% (w/v) sodium azide (pH 6.0) (DTNB assay). Error bars represent the standard deviation from four independent replicates.

dx.doi.org/10.1021/bi401433f | *Biochemistry* 2014, 53, 57−67

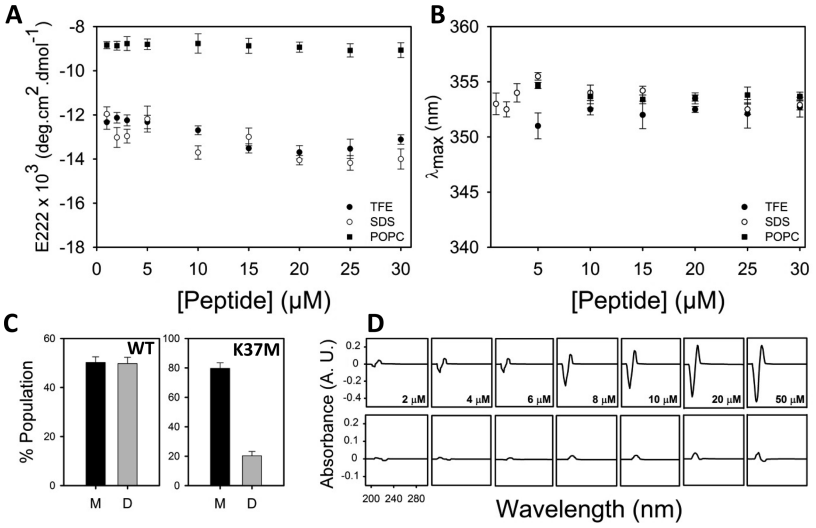

Figure 5. Lys37 mediates the noncovalent dimerization of the CLIC1 TMD peptide via a cation−π interaction. The E_{222} (A) and λ_{max} (B) values from K37M peptide samples incubated in SDS micelles or POPC liposomes show no change at increasing peptide concentrations and are identical to the values of samples incubated in TFE. (C) The monomeric and dimeric forms of 15 μM wild-type (left) and K37M (right) peptides were isolated using SDS−PAGE and band intensities quantified using ImageJ. Removal of Lys37 severely reduces the population of dimeric species compared to the population of the wild type. (D) UV absorption of the wild-type (top) and K37M (bottom) TMD peptides shows that Lys37 forms a cation−π interaction that presumably stabilizes the helical dimer. The negative−positive peak pair at 220/230 nm is considered a marker of tryptophan residues involved in cation−π interactions.[27,28] Error bars represent the standard deviation from four independent replicates.

(K_{SV} = 8.6 M^{-1}) and iodide (K_{SV} = 2.53 M^{-1}) quenching of the K37M peptide yield Stern−Volmer constants that are roughly 2-fold lower than that of either free NATA in solution (16.15 M^{-1} with acrylamide and 3.88 M^{-1} with iodide) or the wild-type peptide (15.35 M^{-1} with acrylamide and 3.52 M^{-1} with iodide). Upon addition of SDS micelles or POPC liposomes, a further 3-fold decrease in acrylamide accessibility occurs. This reduction is 2.5-fold greater for the K37M peptide than for the wild-type peptide (see Table 1). The iodide accessibility of the peptide in the presence of SDS, however, is similar to that of the wild type. This correlates well with data from H_2O_2-induced quenching and indicates that Trp35 (i) is protected from quenching by the micelles and liposomes and (ii) is less solvent accessible in the K37M mutant than in the wild type.[33]

Unlike that of Trp35, the solvent accessibility of Cys24 remains unchanged in the K37M peptide with an ∼35% reduction in the fraction of free thiols following the addition of SDS micelles (Figure 4D and Table 1). In POPC, a dual DTNB assay was employed whereby samples contained either extrinsic DTNB (*cis* face) or DTNB encapsulated within the liposomes (*trans* face). The data shown in Figure 4D suggest that the *trans* configuration is more prominent (∼60%) whereas only 30−35% of the residues react with extrinsic DTNB. This is identical to the case for the wild-type peptide (Table 1) and suggests that the orientation of Cys24 is not affected by the K37M mutation.

Role of Lys37 in Dimerization of the CLIC1 TMD. We have previously demonstrated, using concentration-dependent studies and SDS−PAGE, that the CLIC1 TMD forms stable dimers in membrane mimetics.[19] Panels A and B of Figure 5 show the results of concentration-dependent studies of K37M peptide samples incubated in TFE, SDS, and POPC. Both the E_{222} and λ_{max} values showed little to no change in either SDS or POPC and followed a trend similar to that of the samples incubated in TFE. Because TFE inhibits quaternary interactions,[29] the similar data from the three mimetics suggest that removal of Lys37 has severely impeded self-association of the peptide.

Tricine SDS−PAGE was subsequently used to assess the effect of the mutation on the formation of dimeric TMD (Figure S3 of the Supporting Information). The use of SDS−PAGE to monitor TMD association has been well-documented.[34−37] The K37M mutation has reduced the population of dimeric species by ∼30%, with the majority of the peptide remaining monomeric across all concentrations tested (Figure 5C and Figure S3 of the Supporting Information). The extent of smearing of the peptide band at high concentrations was also reduced relative to that of the wild type (Figure S3 of the Supporting Information). This suggests impaired formation of higher-order oligomers. Like that of the wild-type peptide, the migration patterns were independent of pH, denaturation, and reducing conditions. This agrees well with the reversible thermal denaturation (Figure S1 of the Supporting Information) and suggests that the helix−helix interactions between TMD peptides are noncovalent. The presence of a stabilizing noncovalent cation−π interaction is therefore probable.

To further investigate whether a cation−π interaction is involved in dimerization, the concentration dependence of UV absorption was examined in the wild-type and K37M TMD peptides. This method of detecting cation−π interactions is based on the weakening of B_b tryptophan absorbance (at ∼220 nm) accompanied by a red shift to ∼230 nm in the presence of these interactions.[27,28] The negative−positive peak pair at 220/230 nm is considered a marker of tryptophan residues involved in cation−π interactions.[27,28] Figure 5D compares the difference UV absorption spectra of the wild-type and K37M peptides. The wild-type peptide exhibits a positive peak at ∼230 nm and a weaker negative peak at ∼220 nm. This is consistent with previously described reports of tryptophan residues involved in cation−π interactions.[27,28] In the K37M peptide, the negative−positive peak pair at 220/230 nm is no longer observed. Instead, the spectra resemble those of the TFE control in which helix−helix interactions are absent. This

dx.doi.org/10.1021/bi401433f | *Biochemistry* 2014, 53, 57−67

observation suggests that Lys37 and Trp35 are involved in a cation−π interaction.

Chloride Influx Assay. Given that the single TMD of CLIC1 must oligomerize to form a functional channel, dimerization is likely to play a role in Cl^- conductance. The emission spectra of the liposome-encapsulated chloride-sensitive dye Lucigenin at pH 7.4 and 5.5 at various peptide concentrations are shown in Figure 6. The dye emits maximally

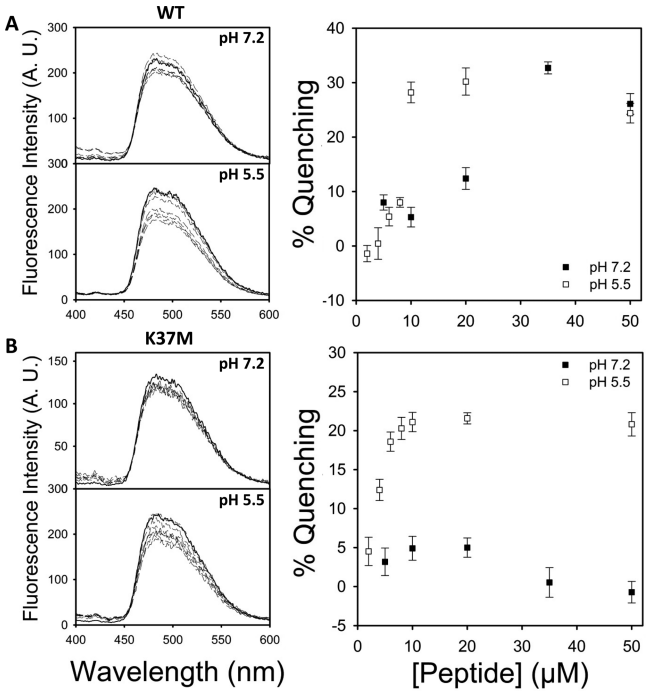

Figure 6. CLIC1 TMD alone is sufficient for chloride ion transport. A chloride influx assay was performed at increasing wild-type (A) and K37M (B) peptide concentrations, based on the quenching of the encapsulated dye Lucigenin. The solid line shows the sample in the absence of peptide, while the dashed lines are samples incubated with 2−50 μM peptide. Removal of Lys37 reduces the efficiency of transport at pH 5.5 and completely eliminates activity at pH 7.2. This is likely a result of (i) disrupted pore formation caused by impaired dimerization coupled with (ii) weakened membrane adsorption at neutral pH. The buffer consisted of 20 mM sodium phosphate, 15 mM potassium chloride, 1 mM DTT, and 0.02% sodium azide (pH 5.5 or 7.2). Error bars represent the standard deviation from four independent replicates.

at 484 nm at both pH values and at all peptide concentrations. Figure 6 shows the percentage quenching of the dye for the wild-type and K37M peptides. The wild-type peptide shows a concentration-dependent increase in the level of dye quenching at both pH values. Maximal quenching (~35%) is achieved between 10−20 μM (pH 5.5) and 30−40 μM (pH 7.2) peptide. The K37M mutation reduces the efficiency of chloride transport by 15% at pH 5.5. At pH 7.2, the K37M peptide shows neither concentration dependence nor significant chloride conductance. The contribution of the methanol solvent was shown to be negligible (Figure S4 of the Supporting Information).

In an attempt to improve our understanding of the mechanism of chloride influx and the role played by dimerization, we investigated the kinetics of chloride influx. Figure 7 shows averaged traces of peptide-mediated quenching of Lucigenin fluorescence. The observed rate constants for

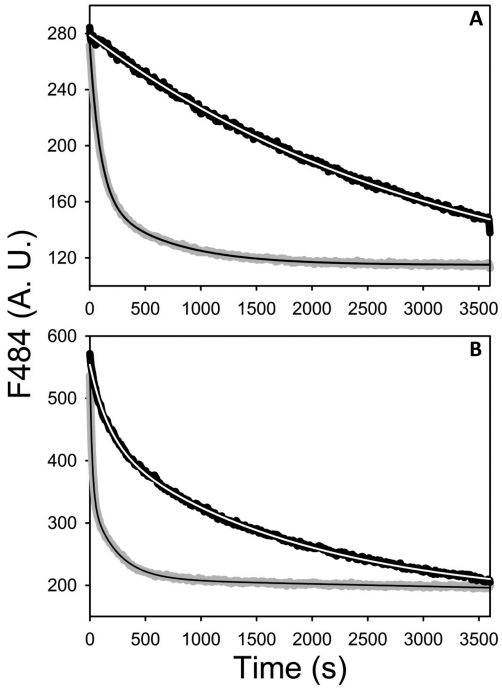

Figure 7. Dimerization modulates the kinetics of chloride influx. The kinetics of chloride influx in the wild-type (gray) and K37M (black) TMD peptides were measured at pH 7.2 (A) and pH 5.5 (B). The curves represent averages of four independent experiments. The data were fit to either a single- or double-exponential decay model using SigmaPlot version 11.0, and fits are shown as solid lines through the data. Removal of Lys37 severely impairs the rate of chloride influx, and the rate is 35-fold (pH 7.2) and 8-fold (pH 5.5) lower than that of the wild type. The buffer consisted of 20 mM sodium phosphate, 15 mM potassium chloride, 1 mM DTT, and 0.02% sodium azide (pH 5.5 or 7.2).

chloride influx (k_{obs}) are listed in Table 2. At pH 7.2, the wild-type peptide displays a two-state mechanism whereas the K37M peptide shows a single state. This is accompanied by an ~35-fold reduction in k_{obs} compared to that of the wild-type peptide. The additional state observed for the wild-type peptide may be attributable to the dimerization process. At pH 5.5, both the wild-type and K37M peptides display a two-state mechanism. The difference in k_{obs} between the wild-type and K37M peptides is reduced to 8- and 2-fold for the two states, respectively. This correlates well with the equilibrium quenching measurements that show that K37M-induced quenching reaches near wild-type levels at pH 5.5.

DISCUSSION

Membrane-bound CLIC1 plays key roles in cell signaling, homeostatic, and apoptotic processes.[38−40] To perform these functions, CLIC1 monomers must insert into membranes and oligomerize to form a chloride ion channel.[21] Despite its physiological relevance, the nature of CLIC1 oligomerization remains poorly understood. Here we report a cation−π interaction implicated in stabilizing the dimeric form of the CLIC1 TMD as it partitions between an aqueous and membrane-mimicking environment. The lysine side chain (Lys37) involved in the interaction was mutated to a methionine, and the resulting changes in the secondary, tertiary, and quaternary structure were observed.

dx.doi.org/10.1021/bi401433f | Biochemistry 2014, 53, 57−67

Table 2. Observed Rate Constants for Peptide-Mediated Chloride Influx[a]

	pH 7.2			pH 5.5		
	k_{obs1} (s^{-1})	k_{obs2} (s^{-1})	R^2	k_{obs1} (s^{-1})	k_{obs2} (s^{-1})	R^2
WT	0.0108 (2.2×10^{-5})	0.0016 (3.7×10^{-6})	0.9994	0.048 (2×10^{-4})	0.0044 (1.1×10^{-5})	0.9986
K37M	0.0003 (8.2×10^{-7})	not available	0.999	0.0058 (3.5×10^{-5})	0.0006 (2.1×10^{-6})	0.9991

[a]Data were fit to either a single- or double-exponential decay model[42] in SigmaPlot version 11.0, from which the observed rate constants (k_{obs}) were derived. The fit error from four independent replicates is given in parentheses.

Lys37 Does Not Direct Folding, Stability, or Membrane Insertion of the CLIC1 TMD. Removal of Lys37 has little impact on the secondary structure of the TMD peptide (Figure 3A,B). In the presence of membrane mimetics, the TMD still undergoes a dramatic structural rearrangement to form an α-helix. This is analogous to the case for the wild type and is consistent with the predicted membrane conformation of the TMD. This residue is therefore unlikely to be involved in the unfolding and/or refolding of the TMD, which is thought to occur at the membrane−cytosol interface.[19,41] The local tertiary structure of the peptide was, however, altered following the removal of Lys37 (Figure 3C). This is not surprising, given the proximity of Lys37 to the lone Trp35 probe. The observed effect can be explained by (i) the introduction of a hydrophobic pocket by methionine or (ii) the lowered local polarity resulting from the removal of Lys37. The latter is of particular interest as there have been several reports of lysine-induced quenching of tryptophan fluorescence when the two residues are involved in a cation−π interaction.[43,44] It is unlikely, however, that removal of Lys37 induces large-scale structural perturbations because the stability of the peptide in membrane mimetics is independent of this residue (Figure S1 of the Supporting Information). Surprisingly, Lys37 remains highly conserved throughout the CLIC family despite being implicated in neither folding nor stability (Figures 1 and 2 and Figure S1 of the Supporting Information). This is compounded by the fact that polar residues are often excluded from transmembrane segments on the basis of their unfavorable energetic contributions in a hydrophobic environment.[45] It is evident, then, that Lys37 must play a specialized role in insertion, oligomerization, and/or function. Fluorescence quenching studies indicate that Lys37 is not, in fact, required for the insertion of the peptide into SDS micelles or POPC liposomes (Figure 4A−C and Figure S7 of the Supporting Information), nor does it affect the orientation of the peptide in these mimetics (Figure 4D). The fact that the wild-type peptide does not show impaired membrane insertion (based on K_{SV} values) relative to those of other peptides lacking polar transmembrane residues[46,47] suggests an alternative role for Lys37.

Lys37 Provides a Driving Force for Helix−Helix Association. The insertion of Lys37 into the membrane requires the energetically unfavorable removal of polar groups from water. To compensate for this, a buried interaction involving Lys37 is likely required. An examination of the structures of several transmembrane domains[48] suggests that when lysine residues are present in transmembrane helices, they rarely occur in regions exposed to membrane lipids. Rather, the amide groups form intra- and interchain contacts with other regions of the peptide.[49] Thus, a buried interaction involving Lys37 may help to direct helix−helix contacts (i.e., oligomerization).

To confirm this theory, we modeled the putative CLIC1 TMD dimer to complement CD, UV, and SDS−PAGE analyses (Figures 2 and 5). The characteristic GxxxG motif[5] found in many transmembrane helical dimers is absent. A study by Doura and Fleming[51] showed that the GxxxG motif is, in fact, neither necessary nor sufficient for dimerization. Rather, the ability of helices to dimerize is governed by complex and detailed interactions at the helix−helix interface.[50] These small residue motifs are replaced by a network of hydrophobic interactions at the dimer interface that presumably contribute to stabilizing the dimeric conformation (Figure 2B). Perhaps most significant was the identification of a putative cation−π interaction between Lys37 and Phe41/Trp35. We validated this finding experimentally and showed that the removal of the lysine cation severely impairs the ability of the TMD to dimerize (Figure 5). The residual dimeric population is likely a result of the hydrophobic contacts (Figure 2B) that maintain weak helix−helix association. A stabilizing cation−π interaction involving Lys37 is therefore likely to play a key role in the dimerization of the CLIC1 TMD peptide. This is particularly relevant taking into account the estimated free energy gain associated with interacting Lys and Trp side chains in a hydrophobic medium (~6 kcal/mol).[16]

Dimerization Modulates the Rate of Cl^- Conductance. Given that CLIC1 contains a single TMD, subsequent oligomerization is required to form a functional pore. This process, which completes the two-step folding model, has been poorly characterized in CLIC1. It is clear that, in the absence of higher-order oligomers, CLIC1 is unlikely to function as a chloride channel. We investigated whether removal of Lys37 and the subsequent disruption of dimerization would impair CLIC1 TMD function. Our data suggest that the wild-type TMD alone is capable of conducting Cl^- ions (Figure 6). This highlights the fact that the CLIC1 TMD is a self-contained structural and functional unit when excised from the full-length protein. Removal of Lys37 does not prevent Cl^- transport but does significantly reduce the efficiency of the process. The retention of hydrophobic helix−helix contacts may explain the ability of the K37M peptide to weakly associate and transport Cl^- ions.

The most noticeable effect of removing Lys37 becomes apparent when analyzing the kinetics of chloride influx (Figure 7). Both the wild-type and K37M peptides showed enhanced activity at low pH. This is consistent with previous reports of the full-length protein[30] in which the pH at the membrane is ~2 units lower than in the cytosol. Lysine ($pK_a \sim 10.5$) is unlikely to undergo changes in its ionized state within the pH range tested. Therefore, the observed rate enhancement at low pH is likely a result of enhanced membrane adsorption resulting from changes in lipid charge. We assume that the rate-limiting step is the insertion and oligomerization of the peptide rather than Cl^- influx. This is the most conservative assumption given that diffusion of Cl^- ion to the pore as well as through the pore is rapid.[52] Hence, the apparent rate constant of Cl^- influx depends on the Gibbs free energies of membrane binding, insertion, and oligomerization. Because binding and insertion do not appear to be altered by the mutation (Figures 3 and 4

dx.doi.org/10.1021/bi401433f | Biochemistry 2014, 53, 57−67

and Figure S7 of the Supporting Information), the difference in the rate of Cl^- influx between the wild-type and K37M peptides is likely a result of oligomerization. Because there are few changes in the kinetics of membrane insertion (Figure S7 of the Supporting Information), we postulate that the decrease in rate is a result of an alteration in the equilibrium of pore formation. With only relatively weak hydrophobic interactions maintaining the dimer, dissociation of the dimer or oligomer would be frequent and the overall rate of chloride transport reduced. Studies by Warton et al.[30] suggest that a CLIC1 dimer may represent a weakly active protopore that subsequently oligomerizes to form the fully active channel. This could describe the observed two-step mechanism of Cl^- influx in the wild-type peptide and explain why the K37M peptide displays only a single step. Such behavior has been observed for other proteins that spontaneously insert into membranes, including diphtheria toxin,[53] Bax,[54] and Bcl-x_L.[55,56] It must be reiterated that the dimer itself is unlikely to represent the functional pore. Rather, it is likely an intermediate step for the formation of higher-order oligomers that then facilitate pore formation. The CLIC1 oligomerization scheme proposed by Singh[20] most closely matches the mechanism suggested by Warton et al.[30] as well as the data presented here. This scheme postulates a two-step process whereby (i) four TMD helices associate to form a protomer and (ii) four protomers interact to form the ion channel. The initial step may be mediated by the cation−π interaction described here, forming a stable and weakly active dimer or tetramer.

Because the cation−π interaction is not required for membrane partitioning or insertion (Figure S7 of the Supporting Information) but is required for Cl^- conductance, it is possible to propose a sequential mechanism for the membrane insertion of the CLIC1 TMD. (i) The unstructured peptide approaches the membrane interface where it refolds to form an α-helix. (ii) The helix partitions onto the membrane surface, followed by spontaneous insertion to form a membrane-spanning helix. (iii) Individual helices associate via a Lys37-mediated cation−π interaction to form dimers. (iv) Dimeric helix bundles associate to form ion channels. This is consistent with the two-step folding model proposed by Popot and Engelman.[2]

In conclusion, the results presented here represent the first study of the interactions that stabilize CLIC1 TMD oligomers in the membrane. We have identified a cation−π interaction involving Lys37 in addition to a network of hydrophobic contacts at the dimer interface. Although this residue is not required for folding, membrane binding, or insertion, it does facilitate CLIC1 TMD self-association. Mutation of Lys37 to Met37 essentially eliminates oligomerization of the membrane-bound peptide. Thus, within a membrane-like environment, interactions involving a polar lysine side chain provide a thermodynamic driving force for helix−helix association. Dimerization, in turn, is required for the effective transport of chloride ions. Further studies will be necessary to define the three-dimensional structure of the CLIC1 TMD, and future work will involve generating high-resolution structural data.

■ ASSOCIATED CONTENT

Supporting Information

Thermal unfolding of the CLIC1 TMD peptide in SDS and TFE (Figure S1), Stern−Volmer plots for acrylamide and iodide quenching (Figure S2), SDS−PAGE gels of the monomeric and dimeric TMD (Figure S3), the effect of methanol on Lucigenin fluorescence (Figure S4), residuals to the fits of the chloride influx kinetic data (Figure S5), contact maps derived from the PREDDIMER analysis of the wild-type and K37M TMD peptide (Figure S6), and membrane insertion kinetic data (Figure S7). This material is available free of charge via the Internet at http://pubs.acs.org.

■ AUTHOR INFORMATION

Corresponding Author

*E-mail: heinrich.dirr@wits.ac.za. Telephone: +27 11 7176352. Fax: +27 11 7176351.

Funding

This work was supported by the University of the Witwatersrand, South African National Research Foundation Grant 68898 to H.W.D., and the South African Research Chairs Initiative of the Department of Science and Technology and National Research Foundation (Grant 64788 to H.W.D.).

Notes

The authors declare no competing financial interest.

■ ABBREVIATIONS

CD, circular dichroism; CLIC1, chloride intracellular channel protein 1; DTNB, 5,5′-dithio-2-nitrobenzoic acid; DTT, dithiothreitol; λ_{max}, maximal emission wavelength; GST, glutathione transferase; HIV, human immunodeficiency virus; NATA, *N*-acetyl-tryptophanamide; POPC, 1-palmitoyl-2-oleoyl-*sn*-glycero-3-phosphocholine; SDS, sodium dodecyl sulfate; TFE, 2,2,2-trifluoroethanol; TMD, transmembrane domain of CLIC1 (residues 24−46).

■ REFERENCES

(1) Overington, J. P., Al-Lazikani, B., and Hopkins, A. L. (2006) How many drug targets are there? *Nat. Rev. Drug Discovery 5*, 993−996.

(2) Popot, J. L., and Engelman, D. M. (1990) Membrane protein folding and oligomerization: The two-stage model. *Biochemistry 29*, 4031−4037.

(3) White, S. H., and Wimley, W. C. (1999) Membrane protein folding and stability: Physical principles. *Annu. Rev. Biophys. Biomol. Struct. 28*, 319−365.

(4) Johnson, R. M., Hecht, K., and Deber, C. M. (2007) Aromatic and cation-π interactions enhance helix-helix association in a membrane environment. *Biochemistry 46*, 9208−9214.

(5) Russ, W. P., and Engelman, D. M. (2000) The GxxxG motif: A framework for transmembrane helix-helix association. *J. Mol. Biol. 296*, 911−919.

(6) MacKenzie, K. R., Prestegard, J. H., and Engelman, D. M. (1997) A transmembrane helix dimer: Structure and implications. *Science 276*, 131−133.

(7) Choma, C., Gratkowski, H., Lear, J. D., and DeGrado, W. F. (2000) Asparagine-mediated self-association of a model transmembrane helix. *Nat. Struct. Biol. 7*, 161−166.

(8) Gratkowski, H., Lear, J. D., and DeGrado, W. F. (2001) Polar side chains drive the association of model transmembrane peptides. *Proc. Natl. Acad. Sci. U.S.A. 98*, 880−885.

(9) Zhou, F. X., Merianos, H. J., Brunger, A. T., and Engelman, D. M. (2001) Polar residues drive association of polyleucine transmembrane helices. *Proc. Natl. Acad. Sci. U.S.A. 98*, 2250−2255.

(10) Ward, S. D., Curtis, C. A., and Hulme, E. C. (1999) Alanine-scanning mutagenesis of transmembrane domain 6 of the M(1) muscarinic acetylcholine receptor suggests that Tyr381 plays key roles in receptor function. *Mol. Pharmacol. 56*, 1031−1041.

(11) Aliste, M. P., MacCallum, J. L., and Tieleman, D. P. (2003) Molecular dynamics simulations of pentapeptides at interfaces: Salt bridge and cation-π interactions. *Biochemistry 42*, 8976−8987.

(12) Kamiyama, T., Miura, T., and Takeuchi, H. (2013) His-Trp cation-π interaction and its structural role in an α-helical dimer of HIV-1 Vpr protein. *Biophys. Chem. 173*−*174*, 8−14.
(13) Dougherty, D. A. (1996) Cation-π interactions in chemistry and biology: A new view of benzene, Phe, Tyr, and Trp. *Science 271*, 163−168.
(14) Waters, M. L. (2002) Aromatic interactions in model systems. *Curr. Opin. Chem. Biol. 6*, 736−741.
(15) Gromiha, M. M. (2003) Influence of cation-π interactions in different folding types of membrane proteins. *Biophys. Chem. 103*, 251−258.
(16) Polyansky, A. A., Volynsky, P. E., Arseniev, A. S., and Efremov, R. G. (2009) Adaptation of a membrane-active peptide to heterogeneous environment. I. Structural plasticity of the peptide. *J. Phys. Chem. B 113*, 1107−1119.
(17) Johnson, J. E., and Cornell, R. B. (1999) Amphitropic proteins: Regulation by reversible membrane interactions (review). *Mol. Membr. Biol. 16*, 217−235.
(18) Harrop, S. J., DeMaere, M. Z., Fairlie, W. D., Reztsova, T., Valenzuela, S. M., Mazzanti, M., Tonini, R., Qiu, M. R., Jankova, L., Warton, K., Bauskin, A. R., Wu, W. M., Pankhurst, S., Campbell, T. J., Breit, S. N., and Curmi, P. M. (2001) Crystal structure of a soluble form of the intracellular chloride ion channel CLIC1 (NCC27) at 1.4-Å resolution. *J. Biol. Chem. 276*, 44993−45000.
(19) Peter, B., Ngubane, N. C., Fanucchi, S., and Dirr, H. W. (2013) Membrane mimetics induce helix formation and oligomerization of the chloride intracellular channel protein 1 transmembrane domain. *Biochemistry 52*, 2739−2749.
(20) Singh, H. (2010) Two decades with dimorphic Chloride Intracellular Channels (CLICs). *FEBS Lett. 584*, 2112−2121.
(21) Goodchild, S. C., Angstmann, C. N., Breit, S. N., Curmi, P. M., and Brown, L. J. (2011) Transmembrane extension and oligomerization of the CLIC1 chloride intracellular channel protein upon membrane interaction. *Biochemistry 50*, 10887−10897.
(22) Canutescu, A. A., Shelenkov, A. A., and Dunbrack, R. L., Jr. (2003) A graph-theory algorithm for rapid protein side-chain prediction. *Protein Sci. 12*, 2001−2014.
(23) Polyansky, A. A., Volynsky, P. E., and Efremov, R. G. (2012) Multistate organization of transmembrane helical protein dimers governed by the host membrane. *J. Am. Chem. Soc. 134*, 14390−14400.
(24) Sreerama, N., and Woody, R. W. (2000) Estimation of protein secondary structure from circular dichroism spectra: Comparison of CONTIN, SELCON, and CDSSTR methods with an expanded reference set. *Anal. Biochem. 287*, 252−260.
(25) Habeeb, A. F. (1972) Reaction of protein sulfhydryl groups with Ellman's reagent. *Methods Enzymol. 25C*, 457−464.
(26) Schagger, H., and von Jagow, G. (1987) Tricine-sodium dodecyl sulfate-polyacrylamide gel electrophoresis for the separation of proteins in the range from 1 to 100 kDa. *Anal. Biochem. 166*, 368−379.
(27) Xue, Y., Davis, A. V., Balakrishnan, G., Stasser, J. P., Staehlin, B. M., Focia, P., Spiro, T. G., Penner-Hahn, J. E., and O'Halloran, T. V. (2008) Cu(I) recognition via cation-π and methionine interactions in CusF. *Nat. Chem. Biol. 4*, 107−109.
(28) Yorita, H., Otomo, K., Hiramatsu, H., Toyama, A., Miura, T., and Takeuchi, H. (2008) Evidence for the cation-π interaction between Cu^{2+} and tryptophan. *J. Am. Chem. Soc. 130*, 15266−15267.
(29) Roccatano, D., Colombo, G., Fioroni, M., and Mark, A. E. (2002) Mechanism by which 2,2,2-trifluoroethanol/water mixtures stabilize secondary-structure formation in peptides: A molecular dynamics study. *Proc. Natl. Acad. Sci. U.S.A. 99*, 12179−12184.
(30) Warton, K., Tonini, R., Fairlie, W. D., Matthews, J. M., Valenzuela, S. M., Qiu, M. R., Wu, W. M., Pankhurst, S., Bauskin, A. R., Harrop, S. J., Campbell, T. J., Curmi, P. M., Breit, S. N., and Mazzanti, M. (2002) Recombinant CLIC1 (NCC27) assembles in lipid bilayers via a pH-dependent two-state process to form chloride ion channels with identical characteristics to those observed in Chinese hamster ovary cells expressing CLIC1. *J. Biol. Chem. 277*, 26003−26011.
(31) Sreerama, N., Venyaminov, S. Y., and Woody, R. W. (2001) Analysis of protein circular dichroism spectra based on the tertiary structure classification. *Anal. Biochem. 299*, 271−274.
(32) Langosch, D., and Arkin, I. T. (2009) Interaction and conformational dynamics of membrane-spanning protein helices. *Protein Sci. 18*, 1343−1358.
(33) Eftink, M. R., and Ghiron, C. A. (1981) Fluorescence quenching studies with proteins. *Anal. Biochem. 114*, 199−227.
(34) Wigley, W. C., Vijayakumar, S., Jones, J. D., Slaughter, C., and Thomas, P. J. (1998) Transmembrane domain of cystic fibrosis transmembrane conductance regulator: Design, characterization, and secondary structure of synthetic peptides m1-m6. *Biochemistry 37*, 844−853.
(35) Melnyk, R. A., Partridge, A. W., and Deber, C. M. (2001) Retention of native-like oligomerization states in transmembrane segment peptides: Application to the *Escherichia coli* aspartate receptor. *Biochemistry 40*, 11106−11113.
(36) Rath, A., Glibowicka, M., Nadeau, V. G., Chen, G., and Deber, C. M. (2009) Detergent binding explains anomalous SDS-PAGE migration of membrane proteins. *Proc. Natl. Acad. Sci. U.S.A. 106*, 1760−1765.
(37) Walkenhorst, W. F., Merzlyakov, M., Hristova, K., and Wimley, W. C. (2009) Polar residues in transmembrane helices can decrease electrophoretic mobility in polyacrylamide gels without causing helix dimerization. *Biochim. Biophys. Acta 1788*, 1321−1331.
(38) Landry, D. W., Akabas, M. H., Redhead, C., Edelman, A., Cragoe, E. J., Jr., and Al-Awqati, Q. (1989) Purification and reconstitution of chloride channels from kidney and trachea. *Science 244*, 1469−1472.
(39) Fernandez-Salas, E., Sagar, M., Cheng, C., Yuspa, S. H., and Weinberg, W. C. (1999) p53 and tumor necrosis factor α regulate the expression of a mitochondrial chloride channel protein. *J. Biol. Chem. 274*, 36488−36497.
(40) Ronnov-Jessen, L., Villadsen, R., Edwards, J. C., and Petersen, O. W. (2002) Differential expression of a chloride intracellular channel gene, CLIC4, in transforming growth factor-β1-mediated conversion of fibroblasts to myofibroblasts. *Am. J. Pathol. 161*, 471−480.
(41) Fanucchi, S., Adamson, R. J., and Dirr, H. W. (2008) Formation of an unfolding intermediate state of soluble chloride intracellular channel protein CLIC1 at acidic pH. *Biochemistry 47*, 11674−11681.
(42) Demchenko, A. P. (2001) Concepts and misconcepts in the analysis of simple kinetics of protein folding. *Curr. Protein Pept. Sci. 2*, 73−98.
(43) Loewenthal, R., Sancho, J., and Fersht, A. R. (1991) Fluorescence spectrum of barnase: Contributions of three tryptophan residues and a histidine-related pH dependence. *Biochemistry 30*, 6775−6779.
(44) Vos, R., and Engelborghs, Y. (1994) A fluorescence study of tryptophan-histidine interactions in the peptide anantin and in solution. *Photochem. Photobiol. 60*, 24−32.
(45) Partridge, A. W., Melnyk, R. A., and Deber, C. M. (2002) Polar residues in membrane domains of proteins: Molecular basis for helix-helix association in a mutant CFTR transmembrane segment. *Biochemistry 41*, 3647−3653.
(46) Vincent, M., Gallay, J., Jamin, N., Garrigos, M., and de Foresta, B. (2007) The predicted transmembrane fragment 17 of the human multidrug resistance protein 1 (MRP1) behaves as an interfacial helix in membrane mimics. *Biochim. Biophys. Acta 1768*, 538−552.
(47) Freitas, M. S., Gaspar, L. P., Lorenzoni, M., Almeida, F. C., Tinoco, L. W., Almeida, M. S., Maia, L. F., Degreve, L., Valente, A. P., and Silva, J. L. (2007) Structure of the Ebola fusion peptide in a membrane-mimetic environment and the interaction with lipid rafts. *J. Biol. Chem. 282*, 27306−27314.
(48) Singh, H., and Ashley, R. H. (2007) CLIC4 (p64H1) and its putative transmembrane domain form poorly selective, redox-regulated ion channels. *Mol. Membr. Biol. 24*, 41−52.
(49) Groebke, K., Renold, P., Tsang, K. Y., Allen, T. J., McClure, K. F., and Kemp, D. S. (1996) Template-nucleated alanine-lysine helices are stabilized by position-dependent interactions between the lysine

side chain and the helix barrel. *Proc. Natl. Acad. Sci. U.S.A. 93*, 4025−4029.
(50) Burba, A. E., Lehnert, U., Yu, E. Z., and Gerstein, M. (2006) Helix Interaction Tool (HIT): A web-based tool for analysis of helix-helix interactions in proteins. *Bioinformatics 22*, 2735−2738.
(51) Doura, A. K., and Fleming, K. G. (2004) Complex interactions at the helix-helix interface stabilize the glycophorin A transmembrane dimer. *J. Mol. Biol. 343*, 1487−1497.
(52) Almeida, P. F., and Pokorny, A. (2009) Mechanisms of antimicrobial, cytolytic, and cell-penetrating peptides: From kinetics to thermodynamics. *Biochemistry 48*, 8083−8093.
(53) Bennett, M. J., Choe, S., and Eisenberg, D. (1994) Refined structure of dimeric diphtheria toxin at 2.0 Å resolution. *Protein Sci. 3*, 1444−1463.
(54) Garcia-Saez, A. J., Mingarro, I., Perez-Paya, E., and Salgado, J. (2004) Membrane-insertion fragments of Bcl-xL, Bax, and Bid. *Biochemistry 43*, 10930−10943.
(55) Thuduppathy, G. R., Craig, J. W., Kholodenko, V., Schon, A., and Hill, R. B. (2006) Evidence that membrane insertion of the cytosolic domain of Bcl-xL is governed by an electrostatic mechanism. *J. Mol. Biol. 359*, 1045−1058.
(56) Thuduppathy, G. R., and Hill, R. B. (2006) Acid destabilization of the solution conformation of Bcl-xL does not drive its pH-dependent insertion into membranes. *Protein Sci. 15*, 248−257.